

Zeno and anti-Zeno polarization control of spin-ensembles by induced dephasing

Gonzalo A. Álvarez,^{1,2} D. D. Bhaktavatsala Rao,³ Lucio Frydman,^{3,*} and Gershon Kurizki^{3,†}

¹Facultad de Matemática, Astronomía y Física, Universidad Nacional de Córdoba, 5000 Córdoba, Argentina.

²Fakultät Physik, Universität Dortmund, Otto-Hahn-Strasse 4, D-44221 Dortmund, Germany.

³Department of Chemical Physics, Weizmann Institute of Science, Rehovot, 76100, Israel.

We experimentally and theoretically demonstrate the purity (polarization) control of qubits entangled with multiple spins, using induced dephasing in nuclear magnetic resonance (NMR) setups to simulate repeated quantum measurements. We show that one may steer the qubit ensemble towards a quasi-equilibrium state of certain purity, by choosing suitable time intervals between dephasing operations. These results demonstrate that repeated dephasing at intervals associated with the anti-Zeno regime lead to ensemble purification, whereas those associated with the Zeno regime lead to ensemble mixing.

PACS numbers: 03.65.Xp, 03.65.Ta, 03.65.Yz, 05.70.Ln

Introduction.— The ability to understand and manipulate the dynamics of “open” quantum systems, *i.e.* systems that interact with their environment (“bath”), is a major challenge for fundamental quantum physics and a prerequisite for novel applications such as quantum heat engines [1], quantum information storage and retrieval [2] and precision measurements [3]. This is particularly true of information-carrying spin-1/2 particles, known as quantum bits (qubits), coupled to spin-1/2 particles of other species that constitute the bath. Such systems are usually controllable by coherent fields [4–7]. Here we address their manipulations by incoherent, random fields that dephase the system and thereby mimic quantum non-demolition (QND) measurements [8, 9]. Such manipulation is conceptually intriguing: whereas QND measurements leave a closed system intact, they can affect an open system, by destroying its correlations (coherences) with the bath. As recently predicted for qubits coupled to thermal oscillator baths, such measurements can steer the qubit ensemble, towards either higher or lower purity (“cooling” or “heating”) [10]: Namely, the qubit does not retain its state as the measurements accumulate, but rather converges to an asymptotic steady state. In the Quantum Zeno (QZE) regime, highly frequent measurements raise the asymptotic excitation and entropy (mixing) of the qubit. This reflects the hitherto unnoticed fact that QZE dynamics equalize the bath-induced upward and downward transition rates, in the qubit. By contrast, less frequent measurements conforming to the anti-Zeno (AZE) regime [10], predominantly enhance downward transitions (relaxation to the ground state) and thus purify (“cool”) the qubit. These predicted measurement-induced changes of the equilibrium go beyond previous studies that focused on transition-rate (relaxation) slowdown in the QZE regime and its speedup in the AZE regime [9] and have been experimentally verified [11].

The present study considers a scenario different from that of Ref. [10]: the interaction of a spin-1/2 or qubit system S with N identical spin-1/2 particles I that constitute its “bath”. Such a situation is encountered in NMR

setups [7], and field-driven quantum dots [12]. Since all the I spins have the same energy levels, such spin-baths are spectrally degenerate, as opposed to the broad spectrum of oscillator baths. The resulting qubit-bath dynamics is therefore different for the two scenarios and hence we ask: do the equilibrium changes predicted in Ref. [10] hold for both scenarios?

In this work we demonstrate that they do, despite their differences: we experimentally lower or raise the purity of the system and bath spins via frequent induced dephasings that simulate QND energy measurements [9] respectively, by timing the dephasing intervals to be in the QZE (evolution slowdown) or AZE (evolution speedup) regime [9] respectively. Remarkably, repeated dephasings at intervals conforming to the AZE lead to highly-effective polarization exchange that can overcome even large frequency detunings (off-resonant mismatch) of the qubit and bath spins and induce polarization transfer that is as large as if it were the Hartmann-Hahn resonant transfer [13]. This novel effect, demonstrated by our NMR polarization transfer experiments, is termed here *incoherent resonance*, as it stems from repeated system-bath correlation erasure (dephasing).

Model and dynamical regimes.— We assume that the qubit-bath system is described by an effective Hamiltonian

$$H = H_0 + H_{SI} + H_M(t). \quad (1)$$

having the following terms: (i) The H_0 Hamiltonian accounts for the coherent evolution of the qubit and the bath; under a Zeeman-like interaction with respective Larmor frequencies ω_S and ω_I . (ii) The H_{SI} term describes the coupling between the S and I spins, chosen for simplicity to be oriented perpendicular to the Zeeman field,

$$H_{SI} = J \sum_k S^x I_k^x, \quad (2)$$

S^x and I_k^x being the σ_x Pauli operators for the respective species. (iii) The time-dependent Hamiltonian $H_M(t)$ involves intermittently switched random fields that mimic repeated QND measurements.

The incoherent S - I cross-polarization transfer that we here discuss is then determined by the interplay between “free” evolution and measurement effects, as follows:

(a) *Free-evolution*: This will be governed by the time-independent terms in Eq. (1). In an interaction picture, *i.e.*, in a “doubly” rotating frame with frequencies ω_S and ω_I , H_{SI} will have contributions from both rotating-wave (*RW* or flip-flop) terms $S^+ I_k^-$, oscillating as $e^{it(\omega_S - \omega_I)}$, and co-rotating (*CR* or flip-flip) terms $S^+ I_k^+$ oscillating as $e^{it(\omega_S + \omega_I)}$, and by their respective Hermitian conjugate terms. It is clear that the short-time initial evolution will be dominated by the rapidly oscillating *CR* terms, and the long-time evolution by their *RW* counterparts. The energy transfer from *I* to *S* due to *CR* and *RW* terms is then governed by the respective population transfer coefficients [14] $P_{CR} = \frac{\tilde{J}^2}{\tilde{J}^2 + (\omega_S + \omega_I)^2}$, $P_{RW} = \frac{\tilde{J}^2}{\tilde{J}^2 + (\omega_S - \omega_I)^2}$, where \tilde{J} is the effective *S*–*I* interaction. At resonance ($\omega_S = \omega_I$), $P_{RW} = 1$, causing a complete exchange of polarization at $t \sim n\pi/J$ ($n = 1, 2, \dots$). In such situations, and given that usually $\omega_S, \omega_I > J$, one can ignore the fast-oscillating *CR* terms and obtain the dynamics using the *RW* terms only [13]. By contrast, under strongly mismatched conditions, *i.e.*, $\omega_S \gg \omega_I$ or vice-versa, $P_{RW} \sim P_{CR}$, and the dynamics is equally dominated by the *CR* and *RW* terms. For such large detuning, the H_{SI} –driven transfer of polarization between the *S* and *I* spins is inhibited: The polarizations of all spins are then locked at their initial values, as $P_{CR} \sim J/|\omega_S + \omega_I|$, $P_{RW} \sim J/|\omega_S - \omega_I| \ll 1$. While the presented results are focused on the given H_{SI} , they are general for Hamiltonians that contain *RW* and *CR* terms.

(b) *Projective measurements*: These will be imparted by brief interactions described by $H_M(t)$ [14]. Each such nonselective (unread) projective measurement [10] erases the off-diagonal (correlations) terms that may have arisen in the joint *S* + *I* density matrix. This is equivalent to subjecting the system to a brief strong dephasing. Although the respective eigenstates of the system and the bath remain unchanged during these measurements, their correlation energy $\langle H_{SI} \rangle$ changes drastically, affecting subsequent evolution [10]. Here, we mimic such projections onto the system’s energy eigenbasis by an NMR “quantum simulator”, *i.e.*, spatially-random magnetic field-gradients that changes over time (see below).

The polarization exchange between the *S*, *I* spins is dramatically altered in the presence of repeated projective measurements at times $n\tau$, ($n = 0, 1, 2, \dots$). To appreciate this we consider initially uncorrelated equilibrium states $\rho_S \otimes \rho_{I1} \otimes \dots \rho_{IN}$, *i.e.* products of the 2×2 density matrices of the *S*–system and each of the N *I*–bath spins that are diagonal in the energy eigenbasis, with populations of the excited spin state being $0 \leq \epsilon_{S(I)} \leq 1/2$ (the corresponding polarizations $P_{S(I)} = 1 - 2\epsilon_{S(I)}$). We then find that $\epsilon_S(t)$ oscillates as the weighted sum (over all possible *I*-spin quantum numbers) of *S* – *I* oscillatory exchange probabilities. This function depends on N , the bath size, and the anisotropy of the spin ensemble [14] but primarily on the time between consecutive dephasings: (i) At very short times $\omega_{S(I)}t \ll 1$, the *S* evolution is

dominated by the fast-oscillating *CR* terms, so that the freely-evolving polarization of the *S* spin is driven away from $(1 - 2\epsilon_S(0))$, causing depolarization of *S* (“heating”): $\epsilon_S(t) < \epsilon_S(0)$. This *CR* “heating” is amplified by the repeated QZE, since *CR* evolution dominates under the QZE condition $(\omega_S + \omega_I)\tau \ll 1$ [14]: measurements or dephasing at intervals $\tau_h \leq 1/\sqrt{J^2 + (\omega_S + \omega_I)^2}$. This condition means that highly frequent measurements broaden the qubit levels to the extent that they become unresolved, equalizing upward and downward transition rates regardless of temperature (Fig. 1a: red circles and Fig. 1b: lower inset). (ii) By contrast, at longer intervals, the *RW* terms increase the polarization (cause “cooling”) of *S*: $\epsilon_S(t) > \epsilon_S(0)$. Such “cooling”, whose condition is $|\omega_S \pm \omega_I|\tau \gtrsim 1$, is amplified by the repeated AZE [10]: measurements or dephasing at intervals $\tau_c \sim 1/\sqrt{J^2 + (\omega_S - \omega_I)^2}$. This comes about since at such intervals the qubit levels are resolved and downward transitions (relaxation) dominate at finite temperature (Fig. 1a: blue upper triangles and Fig. 1b: upper inset). (iii) After a few measurements (see below) the polarization transfer reaches close to the resonant maximum $[\epsilon_I(0)]$ irrespective of the *S* – *I* detuning. These time-scales determine a resonant-like characteristic that can be exploited as shown in Fig. 1. The qubit polarization is then described, within the *RW* domain by Eq. (III.3) in EPAPS [14].

(c) *Quasi-equilibrium*: After a few measurements at suitable τ ’s, the polarization approaches its asymptotic value and hence the system reaches a quasi equilibrium state (see below), with polarization using *RW* terms only

$$\epsilon_S^{qe} = \epsilon_S(0) + \frac{\epsilon_I(0) - \epsilon_S(0)}{2(1 - \epsilon_I(0))}. \quad (3)$$

Depending on the sign of $\epsilon_I(0) - \epsilon_S(0)$, ϵ_S^{qe} can be either larger or smaller than $\epsilon_S(0)$, corresponding to *S*-spin “cooling” or “heating”, as compared to its initial equilibrium value. The value of $(1 - 2\epsilon_S^{qe})$ is the largest obtainable polarization transfer from the *I* spins to the *S* spin, for any size N of the bath. The transfer achieved by the incoherent resonance is thus always greater than 50% of the coherent maximum, $\epsilon_I(0)/\epsilon_S(0)$, and bound by the full coherent maximum obtainable under a resonant transfer.

(d) *Reheating*: Once ϵ_S^{qe} is reached, the state of the total (*S* + *I*) system commutes with the interaction Hamiltonian in the *RW* approximation, $[\rho, H_{SI}] \approx 0$. This means that if no further measurements are performed, the evolution of all the spins is almost frozen (Fig. 1a: green lower triangles). Yet, in a finite bath as measurements continue to be performed, the deviations from Eq. (3) due to the *CR* terms, gradually “re-heat” (depolarize) both the *S* and the *I* spins (Fig. 1b: blue upper triangles). Hence, different desired quasi-equilibrium values of the *S*-polarization can be obtained depending on N , the bath size, and on the number of measurements performed beyond the number needed to attain ϵ_S^{qe} .

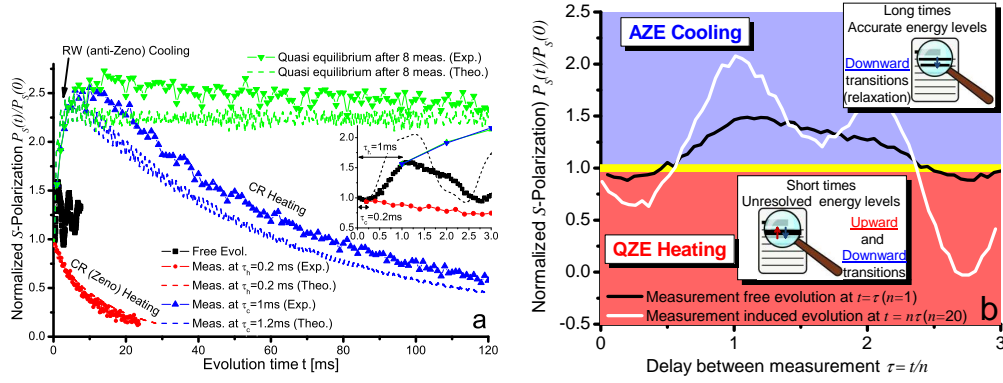


Figure 1: (Color online) Evolution of the S -spin polarization with time. (a) The main panel compares the evolution of the S spin polarization, when interrupted by repeated measurements at intervals of $\tau_c^{exp} = 1$ ms (blue upper triangles) and the evolution interrupted at $\tau_h = 0.2$ ms (red circles), respectively. Also illustrated is the quasi-equilibrium state achieved for the τ_c^{exp} measurements, stopped after 8 ms and followed by free evolution at later times (green lower triangles). The free evolution of the S spin is shown with black squares. The inset zooms the dynamics for short times. These experimental plots are compared with the theoretical curves (dashed lines) obtained by exact diagonalization of the Hamiltonian in Eq. (1) for the experimental parameters above. (b) Schematic representation of the QZE and AZE in thermalized qubits. The white line is the quantum dynamics of the S spin steered by $n = 20$ measurements for varying the time interval τ . It evidences the predicted amplifications compared with the free evolution (black line). For short times (QZE regime), the levels are unresolved so that their transition rates are equal (lower inset), while for long times (AZE regime) they are resolved so that the downward transitions dominate (upper inset).

Results.— The foregoing theoretical predictions which hold for any size of the bath, were tested by liquid state NMR simulators of QND measurement on ^{13}C -methyl iodide (CH_3I) dissolved in CDCl_3 . In liquid-state NMR experiments on the methyl group (CH_3) a ^{13}C spin (S) is J -coupled to a finite “bath” of $N = 3$ equivalent ^1H spins (I) which interact with the S spin but not with each other. The quasi-equilibrium value of polarization obtained for $N = 3$ is $\epsilon_S^{qe} = \epsilon_S(0) + \frac{1}{2} \{(\epsilon_I(0) - \epsilon_S(0))[1 + \epsilon_I(0)(1 - \epsilon_I(0))]\}$. The Hamiltonian in Eq. (1) was reproduced by applying two radio frequency (RF) fields perpendicular to the static field, on resonance with the respective I and S spins. In the doubly rotating frame of the RF fields, precessing with the respective Zeeman frequencies of the spins we then obtain Hamiltonian (1) where the z axis is given by the RF fields direction and the frequencies ω_S and ω_I determined by the strength of the respective RF fields (see [14] for details).

It is essential that both T_1 and T_2 relaxation times are much longer than the time scales used for these quantum simulations.

To mimic the effects of projective measurements, we relied on the use of pulsed magnetic field gradients. Field gradients effectively increase the decoherence rate for correlations in a plane perpendicular to the gradient’s direction, which is along the main B_0 field axis [15]. Yet, it can be shown that repeated application of gradients gives rise to unwarranted temporal correlations in the coherent evolution of the system [14]. In order to realize a sequence of dephasing operations, we resorted to an alternative method that truly simulates projective measurements by applying at regular intervals new, random, values of the field gradi-

ents [14]. In an ensemble average, the correlations are then effectively erased.

The initial conditions are $[1/2 - \epsilon_I(0)]/[1/2 - \epsilon_S(0)] \sim 4$ with the excitations $[1/2 - \epsilon_{I(S)}(0)] \ll 1$. By choosing the time intervals between measurements, to correspond to the QZE or AZE regimes, depolarization (“heating”) or, respectively, polarization (“cooling”) effects predicted by theory were indeed observed under non-matching $\omega_I \sim 250\text{Hz}$ and $\omega_S \sim 420\text{Hz}$ (Fig. 1a) where the choice $|\omega_S - \omega_I|, \omega_S, \omega_I \sim J = 150\text{Hz}$ enhances the predicted effects. Additional measurements performed after attaining the maximum polarization caused re-heating of the S spin by CR terms, as theoretically predicted (blue upper triangles). Finally, by stopping the measurements after maximizing the polarization transfer, we clearly observed the expected quasi-equilibrium behavior of the S -spin (^{13}C) polarization (green lower triangles). Its value agrees well with the theoretically estimated $(1 - 2\epsilon_S^{qe}) \sim 2.9 [1 - 2\epsilon_S(0)]$ considering only the RW term. Its slow decay is a consequence of non-ideal pulses in the implementation of the projective measurements. Excellent agreement is evident between experimental results and numerical simulations without any fitting parameters. Fig. 1b shows the experimental S -polarization steered by $n = 20$ measurements as a function of their time interval τ . Heating (purity loss) or cooling (purity increase) are seen to depend on τ as predicted.

To further explore these incoherent polarization transfer effects, larger detunings $|\omega_S - \omega_I| \gg J$ ($\omega_S \sim 3.5\text{kHz}$ and $\omega_I \sim 2.6\text{kHz}$) and fields $\omega_S, \omega_I \gg J$ were probed and compared with the Hartmann-Hahn resonant [13] NMR transfer (Fig. 2). In these experiments, only

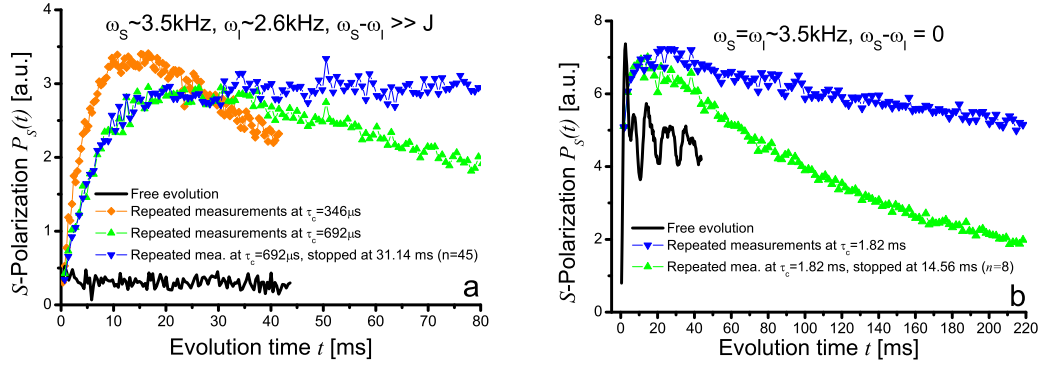


Figure 2: (Color online) Time evolution of the system polarization under matching ($\omega_S = \omega_I$) and off-matching ($\omega_S \neq \omega_I$) conditions. (a). The free evolution (black solid line) of the system (S) spin-polarization, and its evolution interrupted by measurements at time intervals τ of $346\mu\text{s}$ (orange circles) and $692\mu\text{s}$ (green upper-triangles) are shown for off-resonant fields with high detuning. The given τ values were chosen to optimize the transfer. The quasi-equilibrium state corresponding to measurements (at time intervals of $692\mu\text{s}$) stopped after 31.14 ms ($n = 45$), followed by the free evolution for the later times is marked by blue lower triangles. (b). For resonant RF fields, we have plotted the free evolution (black line) of S spin-polarization, evolution interrupted by measurements at time intervals 1.82ms (green upper-triangle). The quasi-equilibrium state corresponding to measurements (at time intervals of 1.82ms) stopped after 14.56 ms ($n = 8$), followed by free evolution at later times, is marked by blue lower triangles. The maximal polarization transfer attained by resonant fields (black line) is almost the same as that achieved and maintained (blue lower triangles) by measurements for all later times.

the I spins were initially excited while the S polarization was completely erased [$\epsilon_S(0) = 1/2$] [14], so that the actual polarization transferred from I to S spin could be determined. Under these off-matching conditions, P_{RW} and P_{CR} were much lower than their resonant values, and the transfer arising from the “free” (uninterrupted) dynamics was negligible (Fig. 2a-solid line). By contrast, the $I \rightarrow S$ polarization transfer achieved by repeated projection measurements was unequivocally evidenced (Fig. 2(a)) to be close to the maximum achievable under resonant conditions (Fig. 2(b)).

Discussion.— The theoretical and experimental data shown in Figs. 1 and 2 clearly demonstrate for the first time the connection between the fundamental Zeno and anti-Zeno effects in frequently measured or dephased open systems and their purity loss or increase, respectively. Measurement (dephasing)-induced transfer of polarization has been shown to be almost as effective as coherent on-resonance transfer, even if the measured system and bath are under presumably unfavorable, off-resonant conditions. We have further demonstrated the ability to steer the system into a quasi-equilibrium, which is maintained when further measurements are stopped.

In terms of their practical use, we envisage potential applications of this non-unitary polarization transfer protocol for qubit purification, required at the initialization stage of quantum information processing [16]. The possibility of increasing the polarization transfer from the pure I spins to the impure S spins even under unavoidable off-resonant conditions could be useful for algorithmic cooling [17]. Hence, the applied and fundamental aspects of the incoher-

ent resonances introduced here merit further exploration.

This work was supported by a Fundacion Antorchas-Weizmann Institute Cooperation grant (# 2530), and the generosity of the Perlman Family Foundation. G.A.A. thanks CONICET and the Alexander von Humboldt Foundation for financial support, and the hospitality of Fakultät Physik, TU Dortmund. Support by EC (MIDAS STREP), ISF, DIP and the Humboldt Research Award is acknowledged by G.K.

* Electronic address: Lucio.Frydman@weizmann.ac.il

† Electronic address: Gershon.Kurizki@weizmann.ac.il

- [1] M. O. Scully, M.S. Zubairy, G.S. Agarwal, and H. Walther, *Science* **299**, 862 (2003).
- [2] J.H. Wesenberg, *et. al.*, *Phys. Rev. Lett.* **103**, 070502 (2009).
- [3] V. Giovannetti, S. Lloyd, and L. Maccone, *Science* **306**, 1330 (2004).
- [4] L. Viola, E. Knill, and S. Lloyd, *Phys. Rev. Lett.* **82**, 2417 (1999).
- [5] G. Gordon, G. Kurizki, and D.A. Lidar, *Phys. Rev. Lett.* **101**, 010403 (2008).
- [6] A. Grelich, *et. al.*, *Nat. Phys.* **5**, 262 (2009).
- [7] R.R. Ernst, G. Bodenhausen, and A. Wokaun, *Principles of Nuclear Magnetic Resonance in One and Two Dimensions*, (Clarendon, Oxford, 1987).
- [8] G. Gordon, *et. al.*, *J. Phys. B* **40**, S61 (2007). V.B. Braginsky and F.Ya. Khalili, *Rev. Mod. Phys.* **68**, 1 (1996).
- [9] A. G. Kofman and G. Kurizki, *Phys. Rev. Lett.* **87**, 270405 (2001); *Nature* **405**, 546 (2000); *Phys. Rev. Lett.* **93**, 130406 (2004).

- (2004).
- [10] N. Erez, *et. al.*, Nature **452**, 724 (2008); G. Gordon, *et. al.*, New J. Phys. **11**, 12302 (2009); G. Bensky, *et. al.*, Physica E **42**, 477 (2010).
- [11] Q. Niu and M. G. Raizen, Phys. Rev. Lett. **80**, 3491 (1998), F. Dreisow, *et. al.*, Phys. Rev. Lett, **101**, 143602 (2008).
- [12] D. Loss and D. P. DiVincenzo, Phys. Rev. A **57**, 120 (1998); P. Maletinsky, A. Badolato, and A. Imamoglu, Phys. Rev. Lett. **99**, 056804 (2007).
- [13] S.R. Hartmann and E.L. Hahn, Phys. Rev. **128**, 2042 (1962).
- [14] See EPAPS Document No. XXXXX for supplementary information. For more information on EPAPS, see <http://www.aip.org/pubservs/epaps.html>.
- [15] L. Xiao and J.A. Jones, Phys. Lett. A **359**, 424 (2006).
- [16] D.P. DiVincenzo, Fortschr. Phys. **48**, 771 (2000).
- [17] J. Baugh, *et. al.*, Nature **438**, 470 (2005).
-

Supplementary information: Zeno and anti-Zeno polarization control of spin-ensembles by induced dephasing

I. QUBIT DYNAMICS WITHIN THE ROTATING WAVE APPROXIMATION

Let us consider the Hamiltonian of Eq. (1) of the main article within the rotating wave approximation, i.e.

$$H_{RW} = \omega_S S^z + \omega_I \sum_k I_k^z + \frac{J}{2} \sum_k [S^+ I_k^- + S^- I_k^+]. \quad (\text{I.1})$$

The total Hamiltonian has a 2×2 block-diagonal structure, each block having a definite value of $S^z + I^z$. Its time-evolution operator has the form

$$U = \sum_{I=0}^{N/2} \sum_{M_I=-I}^I e^{i\phi_{M_I} t} \left\{ \cos \Omega_{M_I} t \hat{\mathcal{L}} + i \sin \Omega_{M_I} t \left[\frac{\Delta}{\Omega_{M_I}} \hat{\sigma}^z + \frac{\tilde{J}_{M_I}}{\Omega_{M_I}} \hat{\sigma}^x \right] \right\} \hat{\mathcal{P}}_I, \quad (\text{I.2})$$

where M_I is the magnetic quantum number of I , $\tilde{J}_{M_I} = J \sqrt{(I - M_I)(I + M_I + 1)}$, $\Delta = (\omega_S - \omega_I)/2$ and $\Omega_{M_I} = \sqrt{\tilde{J}_{M_I}^2 + \Delta^2}$. $\hat{\sigma}$'s are the Pauli operators in the basis of the 2×2 block diagonals of H_{RW} . The projection operator $\hat{\mathcal{P}}_I$ corresponds to each bath-spin sector. The phase ϕ_{M_I} corresponding to each block does not contribute to the dynamics, if the initial state is diagonal in the $S^z + I^z$ basis.

The initial density matrix in the basis of $|\frac{1}{2}; M_I\rangle, |-\frac{1}{2}, M_I + 1\rangle$ is given by

$$\rho_{M_I} = \epsilon_I^{\frac{N}{2} + M_I} (1 - \epsilon_I(0))^{\frac{N}{2} - (M_I + 1)} \begin{bmatrix} \epsilon_S(0)(1 - \epsilon_I(0)) & 0 \\ 0 & \epsilon_I(0)(1 - \epsilon_S(0)) \end{bmatrix}, \quad (\text{I.3})$$

and the diagonal element evolutions are

$$\begin{Bmatrix} ee \\ gg \end{Bmatrix} (t) = \left[1 - \frac{\tilde{J}_{M_I}^2}{\Omega_{M_I}^2} \sin^2 \Omega_{M_I} t \right] \begin{Bmatrix} ee \\ gg \end{Bmatrix} + \frac{\tilde{J}_{M_I}^2}{\Omega_{M_I}^2} \sin^2 \Omega_{M_I} t \begin{Bmatrix} gg \\ ee \end{Bmatrix}. \quad (\text{I.4})$$

Complete exchange of polarization between I to S , i.e. $\epsilon_S(\tau) = \epsilon_I(0)$, is only possible at times τ . This coherent exchange is destroyed in presence of off-resonant fields ($\Delta \neq 0$). In general, the coherent exchange is controlled by the transfer coefficients

$$P_{+-}(n) = \frac{n^2 J^2}{n^2 J^2 + (\omega_S - \omega_I)^2}, \quad 1 \leq n = \sqrt{(I - M_I)(I + M_I + 1)} \leq \sqrt{N}, \quad (\text{I.5})$$

and the spread of the incommensurate frequencies Ω_{M_I} .

A. Counter-rotating terms

When the interaction Hamiltonian has counter-rotating (CR) terms only, i.e.,

$$H_{CR} = \omega_S S^z + \omega_I \sum_k I_k^z + \frac{J}{2} \sum_k [S^+ I_k^+ + S^- I_k^-], \quad (\text{I.6})$$

then $S^z + I^z$ is no longer a conserved quantity. Yet, the Hamiltonian can be expressed in a block-diagonal form in the basis of $|\frac{1}{2}; M_I\rangle, |-\frac{1}{2}, M_I - 1\rangle$. Similarly to the above analysis, the time-evolution of the total system exchange energy between S and I determined by the factor

$$P_{++}(n) = \frac{n^2 J^2}{n^2 J^2 + (\omega_S + \omega_I)^2}. \quad (\text{I.7})$$

II. REPEATED MEASUREMENTS

A measurement on the system which erases its off-diagonal elements while keeping populations unchanged is a nearly ideal quantum-non-demolition (QND) measurement. This measurement projects the system's state onto its energy eigenbasis. In the present case this is also equivalent to projecting also the I -spins on their (total) I_z basis. For the RW and CR interaction dynamics, the projective measurement can be performed individually in each subspace of $S^z + I^z$. By rewriting the initial density matrix in Eq. (I.3) as $\rho_{M_I} = \text{Tr}[\rho_{M_I}] \begin{bmatrix} x_{M_I} & 0 \\ 0 & 1 - x_{M_I} \end{bmatrix}$ and accounting that off-diagonal elements are erased by each projective measurement, if n of them are performed at time-intervals τ , then

$$x_{M_I}(t = n\tau) = f_{1M_I}^n(\tau)x_{M_I} + f_{2M_I}(\tau) \sum_{m=0}^n f_{1M_I}^m(\tau), \quad (\text{II.1})$$

where $f_1(t) = 1 - \frac{2\tilde{J}_{M_I}^2}{\Omega_{M_I}^2} \sin^2 \Omega_{M_I} t$ and $f_2(t) = \frac{\tilde{J}_{M_I}^2}{\Omega_{M_I}^2} \sin^2 \Omega_{M_I} t$. In the limit of $n \rightarrow \infty$, $x_{M_I}(t) = \frac{f_{2M_I}(\tau)}{1 - f_{1M_I}(\tau)} = \frac{1}{2}$ and the density matrix $\rho_{M_I}^{qe} = \rho_{M_I}(t \rightarrow \infty) = \text{Tr}[\rho_{M_I}] \begin{bmatrix} \frac{1}{2} & 0 \\ 0 & \frac{1}{2} \end{bmatrix}$. Hence the total density matrix (qubit + bath) commutes with the Hamiltonian H_{RW} . A similar equilibrium state can be found for the H_{CR} .

III. STEADY-STATE VALUES OF THE QUBIT POPULATIONS

The time-dependent population of the S spin can be found by tracing over the bath degrees of freedom obtaining

$$\epsilon_S(t) = \epsilon_S(0) + \frac{\epsilon_I(0) - \epsilon_S(0)}{1 - \epsilon_I(0)} F(t), \quad (\text{III.1})$$

where $F(t) = \sum_{I, M_I} W_{M_I}^I \sin^2 \Omega_{M_I} t$ and $0 \leq F(t) \leq 1$. The weight function $W_{M_I}^I$ is given by

$$W_{M_I}^I = \lambda_I \epsilon_I(0)^{\frac{N}{2} + M_I} (1 - \epsilon_I(0))^{\frac{N}{2} - M_I} J_{M_I}^2 / \Omega_{M_I}^2, \quad 0 \leq W_{M_I}^I \leq 1, \quad (\text{III.2})$$

where $\lambda_I = \frac{N!}{(N/2+I)!(N/2-I)!} \frac{2I+1}{N/2+I+1}$. By performing repeated measurements as in the above section, the final S -spin polarization within RW approximation is given by

$$\epsilon_S(t = n\tau) = \epsilon_S(0) + \frac{\epsilon_I(0) - \epsilon_S(0)}{1 - \epsilon_S(0)} F_n(\tau), \quad (\text{III.3})$$

where

$$F_n(\tau) = \frac{1}{2(\epsilon_I(0) - \epsilon_S(0))} \sum_{I, M_I} W_{M_I}^I [\{\epsilon_I(0)(1 - \epsilon_S(0)) + \epsilon_S(0)(1 - \epsilon_I(0))\} (1 - f(\tau)) \sum_{m=0}^{n-1} f^m(\tau) - 2\epsilon_S(0)(1 - \epsilon_I(0))(1 - f^n(\tau))]. \quad (\text{III.4})$$

In the above equation $f(\tau) = \cos 2\Omega_{M_I} \tau$. After few measurements $f^n(\tau)$ becomes negligibly small and $\sum_{m=0}^{n-1} f^m(\tau) \sim \frac{1}{1-f(\tau)}$. Then, a steady state value is attained for any bath size N , given by

$$\epsilon_S^{qe} = \epsilon_S(0) + \frac{\epsilon_I(0) - \epsilon_S(0)}{2(1 - \epsilon_I(0))} \left[1 - \sum_I \lambda_I \epsilon_I(0)^{\frac{N}{2} + I} (1 - \epsilon_I(0))^{\frac{N}{2} - I} \right]. \quad (\text{III.5})$$

The equilibrium value for, $N = 3$, can be evaluated from the above equation, giving

$$\epsilon_S^{qe} = \epsilon_S(0) + \frac{1}{2} \{(\epsilon_I(0) - \epsilon_S(0))[1 + \epsilon_I(0)(1 - \epsilon_I(0))]\}. \quad (\text{III.6})$$

Since $0 \leq \epsilon_S(0), \epsilon_I(0) \leq 1$, there will always be a gain in polarization $\epsilon_S^{qe} > \epsilon_S(0)$, if $\epsilon_I(0) > \epsilon_S(0)$. If the interaction Hamiltonian has counter-rotating terms only, the projective equilibrium value is given by

$$[\epsilon_S^{qe}]_{CR} = \epsilon_S(0) + \frac{1}{2} \{(1 - \epsilon_I(0) - \epsilon_S(0))[1 + \epsilon_I(0)(1 - \epsilon_I(0))]\}. \quad (\text{III.7})$$

Thus the counter-rotating terms take $\epsilon_S(0)$ close to $1 - \epsilon_I(0)$.

Large N limit

For large N one can attain the maximum achievable polarization transfer from the bath spins to the qubit (using RW terms only). This saturation value, $\epsilon_S^{qe} \simeq \epsilon_S(0) + \frac{\epsilon_I(0) - \epsilon_S(0)}{2(1 - \epsilon_I(0))}$, is reached for any value of the magnetic fields, ω_S and ω_I .

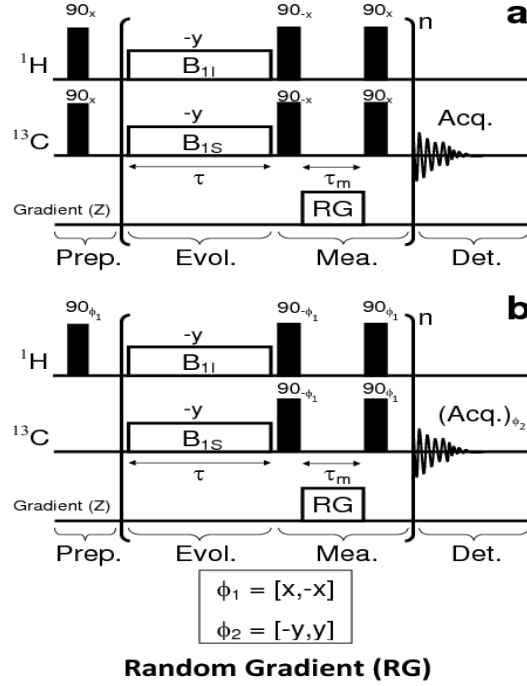


Figure 3: **NMR pulse sequence.** (a) Both kinds of spins are excited for the initial condition (Fig. 1, main text). (b) Based on the phase cycling of pulses and the acquisition process, only the I spins are effectively excited as initial conditions of this variant (Fig. 2, main text). The time length of the 90° pulses were $8\ \mu\text{s}$ for the I spins (^1H) and $15\ \mu\text{s}$ for S (^{13}C). We used for the random intensities of the gradient values in the range $|\Delta B_z| \leq 30\ \text{G cm}$, where the length of the sample is approximately $1\ \text{cm}$. This leads to a variation of the precession frequency around the static field of approximately $125\ \text{kHz}$ for ^1H and $32\ \text{kHz}$ for ^{13}C . The time duration for the gradients is $\tau_m = 100\ \mu\text{s}$, satisfying the condition $\Delta\omega_h\tau_m = \gamma_S\Delta B_z h\tau_m \gg 2\pi$.

IV. EXPERIMENTAL DESCRIPTION OF THE NMR SIMULATOR

A. Hamiltonian realization

The experiment described in the main text involves one spin S and three bath spins I in the presence of a static magnetic field B_0 in the z direction. Considering that the differences of the Larmor frequencies are far greater than the J -coupling between the spins, the effective static Hamiltonian is given by

$$H = \omega_{I0}I^z + \omega_{S0}S^z + JI^zS^z, \quad (\text{IV.1})$$

where $I^z = \sum_k I_k^z$, the sum being over bath spins. When radio-frequency (RF) magnetic fields B_{1I} and B_{1S} oscillating at frequencies ω_{I0} and ω_{S0} are applied, the Hamiltonian in a doubly rotating frame, precessing with the respective Larmor frequencies, becomes [1]

$$H = \omega_I I^y + \omega_S S^y + JI^zS^z, \quad (\text{IV.2})$$

where $\omega_I = \gamma_I B_{1I}$ and $\omega_S = \gamma_S B_{1S}$.

We assume that the direction of the RF fields is $-y$ in this frame. By making a change of variables for the spatial directions ($y \rightarrow z, z \rightarrow x$) this Hamiltonian becomes equivalent to the one given in Eqs. (1) and (2) of the main text,

$$H = \omega_I I^z + \omega_S S^z + J I^x S^x. \quad (\text{IV.3})$$

We would like to note that the presence of both RW and CR terms in the above Hamiltonian is a direct consequence of the anisotropic $I^x S^x$ coupling. The $\vec{I} \cdot \vec{S}$ or $S^x I^x + S^y I^y$ coupling, as found in many natural spin systems, would result only in AZE cooling and quasi-steady state behavior discussed in the main text. The QZE heating and the reheating effects would be absent, because of the cancellation of the CR terms.

B. Pulse sequence with random gradients

Figure 3 is a schematic representation of the NMR pulse sequence used for simulating the measurement-induced quantum dynamics described in the main text. The preparation of the initial state, shown in Fig. 3, consists of the following steps:

(i). 90° RF pulses applied along the x axis [3], exactly on-resonance with the respective Larmor frequencies of both spin species. These pulses rotate the magnetizations from the initial z direction to the $-y$ direction. This is followed by the application of on-resonance RF fields pointing to the $-y$ direction on both kinds of spins, and the Hamiltonian (IV.3) is obtained during time τ .

(ii). In order to simulate the projective measurements, we rotate the polarization back to the z axis by 90° pulses on the $-x$ axis. At this point a static field gradient is applied during time τ_m . To simulate a projective measurement, the gradient intensity is chosen randomly (see section V).

Thus the Hamiltonian generated by the field gradients in a slice of the sample at a position z on the axis parallel to the gradient direction is given by $H_M^z(t) \propto \sum_n (\gamma_S \Delta B_z^n z S_z + \gamma_I \Delta B_z^n z I_z) \theta(t - n\tau) \theta(n\tau + \tau_m - t)$, where ΔB_z^n is the gradient strength at the step n . After each τ_m time, the ensemble average of the different portion of the sample preserves the populations in the density matrix but erases the quantum correlations between the I and S spins. Additionally, the non-diagonal elements of the density matrix within the blocks of constant total spin of I , the so-called zero quantum coherences, are not erased, due to the full chemical equivalence of the I spins.

(iii). Following this projection the polarizations are returned to the $-y$ direction by 90° pulses on the x axis, and the entire cycle is repeated as schematized in Fig. 3. After n cycles, we realize the acquisition of the S_y magnetization as if n projective measurements were performed on S . As the coherences between I spins are not modified by the gradients, the simulated measurements mimic measurements only on the S spin.

(iv). Alternatively one can prepare an initial excitation on the I spins only. For this purpose, during the preparation time, only the I spins are rotated to the $-y$ direction, keeping the S magnetization on the z axis. By phase cycling we cancel out the initial contribution of the S spins (i.e., $\epsilon_S(0) = 1/2$).

C. Pulse sequence without random gradients

In order to compare these evolutions with the free-evolution dynamics, we repeated the experiment with the same pulse sequences but with null gradients. This procedure gives the same time scales for the relaxation and for other non-ideal features of the pulses, but does not modify the free dynamics between measurements. Decoherence is manifest by the reduction of the oscillation amplitude as time goes on. However, the first oscillations are comparable for both procedures. This provides the evidence that there is no polarization transfer during the $\pi/2$ pulses. The polarization control by simulated measurements discussed in the paper is only achieved when the random gradients are introduced to dephase of the coherences (correlations) between S and I spins (Eq. V.2).

V. GRADIENT-DRIVEN PROJECTIVE MEASUREMENTS IN NMR

The experimental simulations of repeated projective measurements were achieved with *random gradient fields*. A brief analysis of this equivalence is given below.

We consider a S spin in presence of a magnetic field on the y axis whose Zeeman frequency is ω_S . Its initial state is $\rho_S = \exp(-\beta\omega_S S^z)/\mathcal{Z} \approx (\mathbf{1} - \beta\omega_S S^z)/\mathcal{Z}$ in the high temperature limit, a typical condition in NMR experiments

[1]. Its evolution is given by

$$\rho(\tau) = S^z \cos(\omega_S \tau) + S^x \sin(\omega_S \tau), \quad (\text{V.1})$$

where we do not write the constant evolution of the identity operator and the factor $-\beta\omega_{0S}/\mathcal{Z}$. By performing projective measurements at time intervals τ on the energy eigenbasis of S^z , $S^x \sin(\omega_S \tau)$ is erased. After n measurements $\rho_n(n\tau) = S^z \cos^n(\omega_S \tau)$. Applying a field gradient on the z axis at time intervals τ during a time τ_m to simulate the measurements, a slice of the sample at position z is affected by the field $\Delta B_z z$, where ΔB_z is the gradient value. The resulting evolution of the slice's density matrix (V.1) is $\rho_z(\tau) = S^z \cos(\omega_S \tau) + [S^x \cos[\Delta\omega_z \tau_m] + S^y \sin(\Delta\omega_z \tau_m)] \sin(\omega_S \tau)$, where $\Delta\omega_z = \gamma_S \Delta B_z z$. Its ensemble average within the sample length h is then $\rho(\tau) = \int_{-h/2}^{h/2} \rho_z(\tau) \frac{dz}{h} = S^z \cos(\omega_S \tau)$, assuming that $\Delta\omega_h \tau_m = \gamma_S \Delta B_z h \tau_m \gg 2\pi$.

While this result represents a projective process for $n = 1$, the next step $n = 2$ is no longer the outcome of two consecutive projections. By calculating the density matrix of the portion z of the sample at this step and considering the ensemble average

$$\rho(2\tau) = \int_{-h/2}^{h/2} \rho_z(2\tau) \frac{dz}{h} = S^z \cos^2(\omega_S \tau) + S^x \sin(\omega_S \tau) \int_{-h/2}^{h/2} [\cos(\omega_S \tau) \cos^2(\Delta\omega_z \tau_m) - \sin^2(\Delta\omega_z \tau_m)] \frac{dz}{h}. \quad (\text{V.2})$$

While the first term on the rhs is equivalent to the one obtained by two projective measurements, but the second term is non-vanishing. In general, correlations of multiple steps, of the form $\cos^m(\Delta\omega_z \tau_m) \sin^l(\Delta\omega_z \tau_m)$ with l and m even numbers, survive the ensemble average, leading to non vanishing deviations from projective measurement. Therefore, a field gradient by itself does not simulate repeated projective measurements. By changing randomly the gradient intensities at consecutive steps, we destroy correlations among different steps upon taking the ensemble average. Thus only the term $S^z \cos^n(\omega_S \tau)$ survive the ensemble average, properly mimicking the projective measurements.

Similar results are obtained once considered the full S - I system. The Hamiltonian $H_M^z(t)$ described in the preceding section dephases $S_{x,y}$ and $I_{x,y}$ terms in the density matrix when the ensemble average on the position z is taken. An ideal projective measurement is performed when all spins along z experiences a random field. A single gradient gives a particular z -dependent phase to spins along the sample. Only when this gradient is randomized further many times such that the sum of the phases accumulated under each gradient vanishes for each spin, one can realize an ideal projective measurement as showed above. However, because the non-diagonal elements of the density matrix within the blocks of constant total spin of I are not erased, due to the full chemical equivalence of the I spins, the simulated measurements mimic measurements only on the S spin.

* Electronic address: Lucio.Frydman@weizmann.ac.il

† Electronic address: Gershon.Kurizki@weizmann.ac.il

[1] C.P. Slichter, *Principles of magnetic resonance*, 2nd ed. (Springer-Verlag, 1992).

[2] I.S. Gradshteyn and I.M. Ryzhik, *Tables of Integrals, Series, and Products* (Academic Press, USA, 1980).

[3] The spatial directions are defined with respect to the doubly rotating frame which precesses with the Larmor frequencies of the spins.